

$^{180}\text{Ta}^{g,m}$ production cross sections from the $^{180}\text{Hf}(p,n)$ reaction

Eric B. Norman*

Physics Division, Argonne National Laboratory, Argonne, Illinois 60439
and Nuclear Physics Laboratory, University of Washington, Seattle, Washington 98195

Timothy R. Renner†

Physics Division, Argonne National Laboratory, Argonne, Illinois 60439

Patrick J. Grant‡

Department of Nuclear Engineering, University of Washington, Seattle, Washington 98195

(Received 9 November 1981)

Cross sections have been determined for the production of the $J^\pi=1^+$ $^{180}\text{Ta}^g$ from the $^{180}\text{Hf}(p,n)$ reaction from measurements of γ rays emitted following the electron capture and β decay of this 8.1-h state. Total ^{180}Ta production cross sections were determined from measurements of the thick-target (p,n) yield. Upper limits on the cross sections for the production of the long-lived $J^\pi=9^-$ $^{180}\text{Ta}^m$ were obtained by subtracting the $^{180}\text{Ta}^g$ cross sections from the total (p,n) cross sections. These measurements are compared with the results of a statistical-model evaporation calculation.

NUCLEAR REACTIONS $^{180}\text{Hf}(p,n)$, $E_p=6.5-9.0$ MeV; measured total (p,n) cross section, $^{180}\text{Ta}^g$ cross section; deduced $^{180}\text{Ta}^m$ cross section; statistical model calculation. Enriched target. Ge(Li) detector. Neutron detector.

I. INTRODUCTION

It is generally believed that the great majority of the naturally occurring nuclei heavier than iron are synthesized in stars via the slow (*s*) and/or the rapid (*r*) neutron capture processes.¹ Of those nuclei which cannot be produced by either of these mechanisms, many are thought to be synthesized by the proton (*p*) process.¹ ^{180}Ta is a rare odd-odd isotope that is an interesting exception to the above generalizations. Although it is β unstable, its half-life is greater than 2.8×10^{13} years.² The natural abundance of ^{180}Ta relative to ^{181}Ta is 1.2×10^{-4} (Ref. 3).

As can be seen in Fig. 1, ^{180}Ta is bypassed in the *s* process and is shielded from the *r* process by the stability of ^{180}Hf . (However, for a possible way around this obstacle, see the recent work of Beer and Ward.⁴) Furthermore, it is shielded from the conventional *p* process by the stability of ^{180}W . In order to account for the observed abundance of ^{180}Ta , several possible production mechanisms have been proposed. Among these are proton-induced

spallation reactions on abundant heavier nuclei,^{5,6} the $^{181}\text{Ta}(\gamma,n)^{180}\text{Ta}$ reaction,⁷ and the $^{180}\text{Hf}(p,n)^{180}\text{Ta}$ reaction.^{6,8} Measurements of the cross sections for each of these mechanisms would help to decide which, if any, are the major contributors to the observed ^{180}Ta . However, there is an ad-

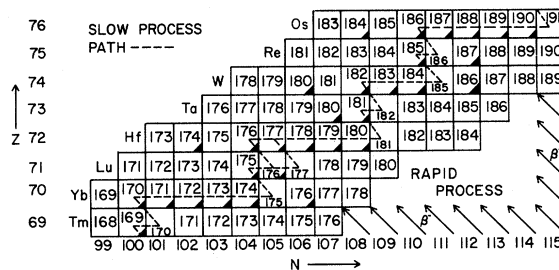


FIG. 1. Expected paths of the slow (*s*) and rapid (*r*) neutron capture processes near $A=180$. Stable nuclei are indicated by shaded triangles. ^{180}Ta is bypassed in the *s*-process and is shielded from the *r* process by the stability of ^{180}Hf . ^{180}Ta is also shielded from the conventional proton (*p*) process by the stability of ^{180}W .

ded complication. Recently it was shown that the ground state of this nucleus, $^{180}\text{Ta}^g$, is not the long-lived naturally occurring state, but in fact is the $J^\pi=1^+$ level which decays to ^{180}Hf and ^{180}W with a half-life of 8.1 h. The long-lived state has been found to be a $J^\pi=9^-$ level at approximately 80 keV excitation energy.⁹⁻¹¹ Thus any ^{180}Ta formed in the short-lived ground state will not contribute to the observed natural abundance of ^{180}Ta .

From the preceding discussion, it is apparent that in order to decide among the various proposed ^{180}Ta production mechanisms an important consideration is the relative production cross sections for the short-lived and long-lived ^{180}Ta states. To date, however, only rough estimates have been made for the values of these cross sections.⁶ In the present experiment we measured the production cross sections and thick-target yields of the 8.1 h $^{180}\text{Ta}^g$ from the $^{180}\text{Hf}(p,n)$ reaction. Total $^{180}\text{Ta}^{g+m}$ production cross sections have been determined from measurements of the thick-target(p,n) yield. Upper limits on the cross sections for the production of the long-lived $^{180}\text{Ta}^m$ have been determined by subtracting the $^{180}\text{Ta}^g$ cross sections from the total ^{180}Ta cross sections. These measurements are compared with the results of a statistical model evaporation calculation.

II. EXPERIMENTAL METHOD

The thick-target yield of $^{180}\text{Ta}^g$ from the $^{180}\text{Hf}(p,n)$ reaction was determined by bombarding 93.86% enriched ^{180}Hf targets with 8.00, 8.50, and 9.00 MeV protons. Each target assembly consisted of a ^{180}Hf disk 0.48 cm in diameter and 0.13 cm thick mounted in an aluminum holder. At the bombarding energies used in the present experiment, the proton beam is completely stopped well within the Hf disk. A separate target assembly was used for each of the three bombarding energies that were used. Beam currents of approximately 25 nA of protons were provided by the Argonne National Laboratory FN tandem accelerator. The proton beam was well collimated to insure that the target and not the holder was struck by the beam. The target assembly was mounted against the end of a 50 cm section of beam tube that was electrically insulated from the rest of the beam line. This 50 cm section of tube thus served as a Faraday cup by which the proton charge was measured with a current integrator.

Each target was bombarded for 5 min and then removed to a remote counting room. To allow for

the decay of any 9.3-min ^{178}Ta produced on the ^{178}Hf contaminant in the target, the initial counting of each target did not begin until 2 h after bombardment. Delayed x rays and γ rays were observed with a 39-cm³ semiplanar Ge(Li) detector. The targets were counted in close geometry using a target holder which permitted accurate and reproducible positioning of the targets in front of the detector.

Each target was counted for 5 min at 1-h intervals over a period of 15 h (roughly two $^{180}\text{Ta}^g$ half-lives). For each counting period a 2048-channel spectrum was accumulated and written on magnetic tape for subsequent off-line analysis. Separate scaling of a pulser, gated by the busy signal from the analog-to-digital converter, provided dead-time information. The overall energy resolution was approximately 1.2 keV (full width at half maximum) for the 122-keV line of ^{57}Co . Energy and efficiency calibrations were performed using standard γ -ray sources.

Measurements of the thin-target $^{180}\text{Ta}^g$ production cross sections were performed with the University of Washington FN tandem accelerator. Natural Hf and 93.86% enriched ^{180}Hf targets of approximately 500 $\mu\text{g}/\text{cm}^2$ areal density were bombarded with approximately 400 nA of protons at energies from 6.5 to 10.0 MeV in 0.5 MeV steps. Two separate sets of measurements were made in which the bombardment time was for either 15 or 30 min. The beam current and target thickness were monitored by a silicon surface barrier detector placed at 35° where the proton elastic scattering followed the Rutherford law. The measured geometric solid angle of the detector agreed well with the results of measurements made using proton elastic scattering from a Au target of known thickness. The monitor yield along with the solid angle information allowed an absolute cross section measurement to be made. Following the bombardments, the targets were transferred to a shielded location and were each counted at least twice with a 7 cm³ planar Ge(Li) detector as described above.

The thick-target total (p,n) yield from ^{180}Hf was measured with a large neutron detection system, the details of which will be described elsewhere.¹² Briefly, the system consists of ten ^3He -filled proportional counters that are imbedded in a 1.5 m diameter graphite moderator which surrounds the target area. The detectors are oriented perpendicular to the beam direction and are positioned around the surface of a half-cylinder. The beam is stopped in the target assembly and the outgoing neutrons are moderated in a 15 cm diameter iron sphere immediately surrounding the target and then in the large

graphite pile. The system's detection efficiency as a function of neutron energy was determined with neutrons produced by the $^7\text{Li}(p,n)^7\text{Be}$ reaction for which the differential and total cross sections are well known.¹³ These measurements showed that the efficiency of the system is (5.5 ± 0.3) percent over the range of neutron energy $0.01 \leq E_n \leq 2.7$ MeV.

The target assembly used in this experiment consisted of a 93.86% enriched ^{180}Hf disk 1 cm in diameter and 0.025 cm thick which was mounted on the end of a 1.3 cm-long graphite plunger. Proton beams were provided by the University of Washington FN tandem accelerator. The thick-target total $^{180}\text{Hf}(p,n)$ yield was measured at energies of 6.5–9.0 MeV in 0.5 MeV steps. The $^{180}\text{Hf}(p,n)$ yield could not be measured at higher energies because of the contributions of other neutron-producing reaction channels, e.g., $^{180}\text{Hf}(p,2n)$.

As a check on our activation technique, we bombarded a thick ^{197}Au target with 9.0 MeV protons to produce $^{197}\text{Hg}^g$ and $^{197}\text{Hg}^m$ via the (p,n) reaction. The yield of $^{197}\text{Hg}^m$ was determined by measuring the number of 134 keV γ rays produced by the internal conversion decay of this state during two counting periods separated by 13 h. Combining our measured isomer yield with previously published values of the ^{197}Hg isomer/g.s. production ratio from the $^{197}\text{Au}(p,n)$ reaction,¹⁴ we calculated the total (p,n) yield from ^{197}Au . Our result of 106 ± 27 neutrons per 10^7 incident protons agrees very well with the value 111 ± 22 obtained by Elwyn *et al.*¹⁵ We also checked our neutron detection system by measuring the thick target (p,n) yields from Cd, Ta, and Pb targets each at three different bombarding energies. The results of these measurements agreed to within $\pm 2.5\%$ of those obtained by Elwyn *et al.*¹⁵ for these targets, thus confirming the present technique.

III. RESULTS

Figure 2 illustrates the x ray and γ -ray spectrum observed following the bombardment of an enriched thick ^{180}Hf target with 8.00 MeV protons. This spectrum was constructed by summing the spectra from nine 5-min counting periods obtained over an 11-h period. The Hf K x rays are produced by several mechanisms: electron-capture decay of $^{180}\text{Ta}^g$ to the 93.3 keV (2^+) ^{180}Hf level, electron-capture decay of $^{180}\text{Ta}^g$ to the (0^+) ^{180}Hf ground state, internal conversion from the 93.3 keV (2^+) ^{180}Hf level, electron-capture decays of other Ta isotopes produced in the target, and fluorescence of the

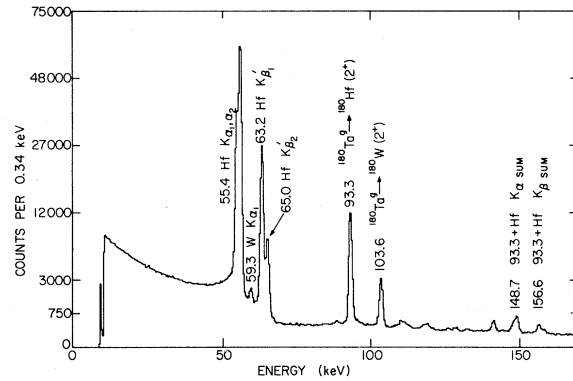


FIG. 2. X ray and γ -ray spectrum observed from the decay of $^{180}\text{Ta}^g$. Small unlabeled peaks are from the decays of other Ta isotopes produced by (p,n) reactions on contaminant Hf isotopes present in the target.

Hf target by γ -rays. The W K x rays are produced from the internal conversion of the 103.6 keV (2^+) ^{180}W level. The 93.3 keV γ -ray arises from the electron-capture decay of $^{180}\text{Ta}^g$ to the first 2^+ level in ^{180}Hf . There is also a small (0.3%) contribution to this peak from the decay of the 2.2 h $^{178}\text{Ta}^m$ produced on the ^{178}Hf contaminant in the target. The 103.6 keV peak is produced by the β^- decay of $^{180}\text{Ta}^g$ to the first 2^+ level in ^{180}W . Small unlabeled peaks are due to the decays of other Ta isotopes.

For the isotopically enriched ^{180}Hf targets, background-corrected yields of the 93.3 and 103.6 keV γ rays were calculated from the data obtained in each counting period. In the case of the thin natural Hf targets, 93 keV γ rays produced by the decays of other Ta isotopes made the use of this γ ray inappropriate. For these targets, only the yields of the 103.6 keV line were used in determining the $^{180}\text{Ta}^g$ production cross sections. These yields were then corrected for decay both during and after bombardment. The number of $^{180}\text{Ta}^g$ nuclei produced were then calculated using the $^{180}\text{Ta}^g$ decay branching ratios and internal conversion coefficients of Ryves.¹⁶

To extract $^{180}\text{Ta}^g$ yields from the thick-target activation measurements, the effects of γ -ray attenuation within the target had to be considered. Using the attenuation coefficients of Storm and Israel¹⁷ and our estimates of the distribution of activity within the thick targets, the attenuations of the γ -rays were calculated for each of the three bombarding energies. The largest attenuation, which occurred for the 93.3 keV γ -ray, amounted to approximately 16% at the 9 MeV bombarding energy.

The relationship between the thick-target reaction

yield and the reaction cross section is

$$Y(E_b) = \int_{E_{th}}^{E_b} \frac{\sigma(E)dE}{(dE/dx)}; \quad (1)$$

thus,

$$\sigma(E_b) = \left[\frac{dY(E)}{dE} \right] \left[\frac{dE}{dx} \right] \Big|_{E=E_b}, \quad (2)$$

where E_{th} is the reaction threshold, E_b is the bombarding energy, and dE/dx is the stopping power of the target. The results of the (p,n) yield measurements are summarized in Table I. The second and third columns of the table are, respectively, the $^{180}\text{Ta}^{g+m}$ and $^{180}\text{Ta}^g$ yields determined from the thick-target measurements. The fourth column represents the thick-target $^{180}\text{Ta}^g$ yield obtained by inserting our measured thin-target $^{180}\text{Ta}^g$ cross sections into Eq. (1) and performing a numerical integration. Reasonable agreement is observed between the results obtained from the thick and thin targets, although the 9.0 MeV points differ by slightly more than one standard deviation.

These yields have been corrected for the effects of the other Hf isotopes contained in the enriched ^{180}Hf target. These corrections varied from the maximum of 5% at 6.5 MeV to 1% at 9.0 MeV. The $^{180}\text{Ta}^g$ yield represents the number of ^{180}Ta ground-state nuclei that result from the neutron emission and any subsequent γ decay. The total (p,n) yield, which is the total ^{180}Ta yield, is the sum of the yields of the short-lived ^{180}Ta ground state and long-lived isomer. At $E_p = 9.0$ MeV it appeared that the $(p,2n)$ reaction began to contribute to the observed neutron yield. An estimate of this contribution indicated that the observed neutron yield at this energy should be reduced by approximately 3.4% to correct for this effect. The corrected value is listed in Table I. While the differences are not great and the uncertainties are substantial, an upper

limit of approximately 10% can be established for the fraction of the $^{180}\text{Hf}(p,n)$ yield that ultimately ends up in $^{180}\text{Ta}^m$.

In order to obtain cross sections from the neutron yield measurements, a least-squares fitting procedure was applied to the yield data. A third order polynomial in the bombarding energy was found to give a good fit to the data. This polynomial was then differentiated and combined with the stopping power values of Anderson and Ziegler¹⁸ to obtain the total ^{180}Ta production cross sections. These results are shown in Table II along with the $^{180}\text{Ta}^g$ cross sections obtained from the thin-target activation experiment. The $^{180}\text{Ta}^g$ cross sections may be subtracted from the $^{180}\text{Ta}^{g+m}$ cross sections to obtain the cross sections for the production of $^{180}\text{Ta}^m$. Because of the small differences between $\sigma(^{180}\text{Ta}^{g+m})$ and $\sigma(^{180}\text{Ta}^g)$ and the relatively large experimental uncertainties, we interpret these differences as upper limits on the $^{180}\text{Ta}^m$ cross sections. These results are summarized in Table II along with values for $\sigma(^{180}\text{Ta}^m)$ which were calculated using a Hauser-Feshbach technique described below.

IV. CALCULATIONS

A Hauser-Feshbach calculation was made of the cross sections for producing the long lived (9^-) and short lived (1^+) states in ^{180}Ta via the (p,n) reaction on ^{180}Hf . The statistical model code STATIS¹⁹ was modified to calculate the total cross sections for forming the ^{180}Ta nucleus in a state of angular momentum J by integrating over excitation energies all states with the given J . In addition, the level density subroutines from the program CASCADE²⁰ were incorporated into the program. At the sub-Coulomb energies studied in the present experiments, inelastic cross sections comprise a small por-

TABLE I. Results for the $^{180}\text{Ta}^{g+m}$ yields and $^{180}\text{Ta}^g$ yields from the $^{180}\text{Hf}(p,n)$ reaction.

E_p (MeV)	$^{180}\text{Ta}^{g+m}$	$^{180}\text{Ta}^g$	$^{180}\text{Ta}^g$
	yield ^a per 10^7 protons	yield ^a per 10^7 protons	deduced yield ^b per 10^7 protons
6.5	4.53 ± 0.23		
7.0	12.3 ± 0.6		
7.5	29.3 ± 1.5		
8.0	61.6 ± 3.1	55.9 ± 5.6	53.4 ± 4.2
8.5	118.5 ± 5.9	112.1 ± 11.2	99.1 ± 7.0
9.0	212.3 ± 12.7	201.9 ± 20.2	160.9 ± 11.4

^aYields determined from thick-target measurements.

^bYields determined from thin-target measurements by use of Eq. (1).

TABLE II. Results for the $^{180}\text{Ta}^{g+m}$, $^{180}\text{Ta}^g$, and $^{180}\text{Ta}^m$ production cross sections for the $^{180}\text{Hf}(p,n)$ reaction.

E_p (MeV)	$^{180}\text{Ta}^{g+m}$ production cross section (mb)	$^{180}\text{Ta}^g$ production cross section (mb)	Upper limit on $^{180}\text{Ta}^m$ production cross section ^a (mb)	$^{180}\text{Ta}^m$ calculated production cross section ^b (mb)
6.5	7.1 ± 0.6	5.8 ± 0.5	1.3	0.5
7.0	15.7 ± 1.4	13.5 ± 1.1	2.2	1.2
7.5	30.7 ± 3.1	25.7 ± 2.0	5.0	2.6
8.0	53.6 ± 5.9	45.6 ± 3.7	8.0	4.9
8.5	87.3 ± 10.8	66.4 ± 5.2	20.9	8.7
9.0	136.1 ± 21.2	79.9 ± 7.0	56.2	14.5

^aObtained by subtracting $\sigma(^{180}\text{Ta}^g)$ from $\sigma(^{180}\text{Ta}^{g+m})$.

^bObtained from Hauser-Feshbach calculations described in text.

tion of the total reaction cross section, and the only reaction energetically favorable is the (p,n) reaction. Thus, the (p,n) reaction cross section was assumed to equal the total reaction cross section. The (p,n) channel was consequently the only one taken into account in the calculation. The proton and neutron transmission coefficients $T_L(E)$ used in the calculation were determined from an optical model calculation performed with the computer code ABACUS²¹ at proton energies from 6.5 to 9.0 MeV in 0.5 MeV steps and at neutron energies from 0.5 to 15 MeV in 0.5 MeV steps. The optical model parameters of Perey²² were used.

By assuming that final states of angular momentum $J < 5$ decay via a gamma cascade to the short lived (1^+) state while those with $J \geq 5$ decay to the long lived (9^-) state, total cross sections for producing these two states were obtained. Different choices for the dividing line between spin states which eventually decay to $^{180}\text{Ta}^g$ or $^{180}\text{Ta}^m$ were found to yield results which were in serious disagreement with the experimental data. These calculations thus can provide an estimate of the $^{180}\text{Ta}^m$ production cross sections expected from the $^{180}\text{Hf}(p,n)$ reaction. In Fig. 3, the calculated total ^{180}Ta , $^{180}\text{Ta}^g$, and $^{180}\text{Ta}^m$ cross sections are compared with the experimental results. The calculated $^{180}\text{Ta}^m$ cross sections are also indicated in Table II.

V. DISCUSSION

A number of authors^{23,24} have discussed the possibility of ^{180}Ta production via proton irradiations that may have occurred during the early stages of the solar system. It has also been suggested that ^{180}Ta might be produced through the interaction of

galactic cosmic rays with nuclei in the interstellar medium.^{5,6} The measured values of the $^{180}\text{Ta}^g$ production cross sections and the upper limits on the $^{180}\text{Ta}^m$ cross sections may help to determine if the $^{180}\text{Hf}(p,n)$ reaction plays a role in the nucleosynthesis of the long-lived $^{180}\text{Ta}^m$.

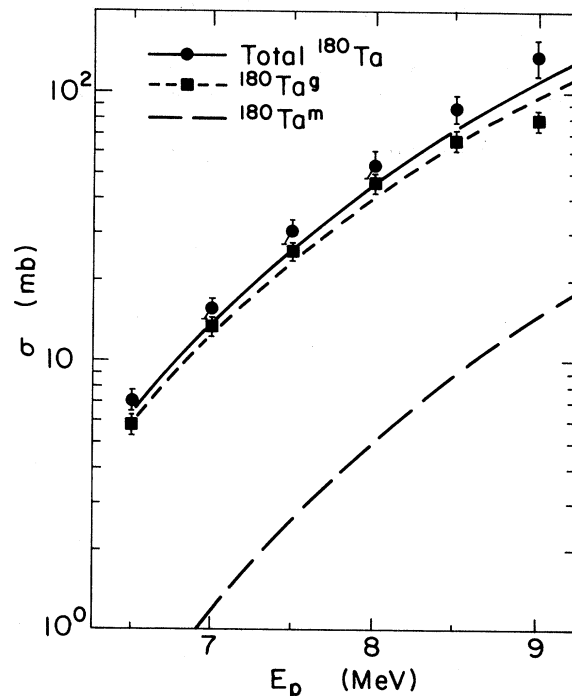


FIG. 3. Circles represent total ^{180}Ta production cross sections and squares represent $^{180}\text{Ta}^g$ production cross sections from the $^{180}\text{Hf}(p,n)$ reaction. The solid, short-dashed, and long-dashed curves are the results of the Hauser-Feshbach calculations for the total ^{180}Ta , $^{180}\text{Ta}^g$, and $^{180}\text{Ta}^m$ production cross sections, respectively.

ACKNOWLEDGMENTS

We wish to thank D. N. Schramm for calling our attention to the interesting problem of ^{180}Ta . J. P. Schiffer's comments and suggestions regarding this

work were most helpful. We thank C. N. Davids and D. F. Geesaman for careful readings of the manuscript. This work was supported in part by the U. S. Department of Energy.

*Present address: Nuclear Physics Laboratory, GL-10, University of Washington, Seattle, WA 98195.

†Present address: Nuclear Science Division, Bldg. 70-A, Lawrence Berkeley Laboratory, Berkeley, CA 94720.

‡Present address: The Boeing Company, Seattle, WA 98031.

¹E. M. Burbidge, G. R. Burbidge, W. A. Fowler, and F. Hoyle, *Rev. Mod. Phys.* **29**, 547 (1957).

²E. B. Norman, *Phys. Rev. C* **24**, 2334 (1981).

³A. G. W. Cameron, *Space Sci. Rev.* **15**, 121 (1973).

⁴H. Beer and R. A. Ward, *Nature* **291**, 308 (1981).

⁵J. Audouze, *Astron. Astrophys. J.* **8**, 436 (1970).

⁶K. L. Hainebach, D. N. Schramm, and J. B. Blake, *Astrophys. J.* **205**, 920 (1976).

⁷K. Ito, *Prog. Theor. Phys.* **26**, 990 (1961).

⁸H. Mabuchi and A. Masuda, *Nature* **226**, 338 (1970).

⁹A. H. Wapstra and K. Bos, *At. Data Nucl. Data Tables* **20**, 16 (1977).

¹⁰E. Warde, thesis, Universite Louis Pasteur de Strasbourg, 1979; E. Warde *et al.*, *J. Phys. Lett.* **40**, L-1 (1979).

¹¹K. S. Sharma *et al.*, *Phys. Lett.* **91B**, 211 (1980).

¹²P. J. Grant *et al.* *Nucl. Instrum. Methods* (to be published).

¹³H. Liskien and A. Paulsen, *At. Data Nucl. Data Tables* **15**, 57 (1975).

¹⁴R. Vandenbosch and J. R. Huizenga, *Phys. Rev.* **120**, 1313 (1960).

¹⁵A. J. Elwyn, A. Marinov, and J. P. Schiffer, *Phys. Rev.* **145**, 957 (1966).

¹⁶T. B. Ryves, *J. Phys. G* **6**, 763 (1980).

¹⁷E. Storm and H. I. Israel, *Nucl. Data Tables* **A7**, 616 (1970).

¹⁸H. H. Andersen and J. F. Ziegler, *The Stopping Powers and Ranges of Ions in Matter* (Pergamon, New York, 1977), Vol. 3.

¹⁹R. G. Stokstad, Wright Nuclear Structure Laboratory, Yale University, Internal Report No. 52, 1972.

²⁰F. Puhlhofer, *Nucl. Phys.* **A280**, 267 (1977).

²¹E. H. Auerbach, BNL Report 23001, 1977.

²²F. G. Perey, *At. Data Nucl. Data Tables* **17**, 1 (1976).

²³D. D. Clayton, E. Dwek, and S. E. Woosley, *Astrophys. J.* **214**, 300 (1977).

²⁴T. Lee, *Astrophys. J.* **224**, 217 (1978).